

The graph automorphism group of the dissociation microequilibrium of polyprotic acids

Nicolás Salas, Justin López, and Carlos A. Arango*

Department of Pharmaceutical and Chemical Sciences, Universidad Icesi, Cali, Colombia

E-mail: caarango@icesi.edu.co

Abstract

The dissociation micro-states (DMSs) of an N -protic acid are described using set theory notation, which facilitates the mathematical description of the dissociation micro-equilibrium (DME). In particular, the DME constants are easily obtained in terms of the dissociation equilibrium constants and the molar fractions of the DMSs. Representing of the DMEs in terms of graph theory allows to identify permutations between DMSs that preserve the vertex-edge connectivity of the graph. These permutations, along with their compositions, led to the identification of the direct product $C_2 \times S_N$ of the cyclic group C_2 , and the symmetric group S_N , as the graph automorphism group of the microdissociation of N -protic acids for $N = 1, 2, \dots, 6$. In this context the microdissociations are associated with the C_2 group while the tautomerizations are related to the S_N group.

1 Introduction

Chemical applications of graph theory have origin in the earlier works on the enumeration of chemical isomers [1–7] and the depiction of molecules [6, 8]. To date, there are numerous chemical applications of graph theory in research fields such as biochemistry, chemical

kinetics, catalysis, quantum chemistry, NMR spectroscopy, chemoinformatics, and new drug discovery, among others [9–13]. In chemoinformatics, graph theory has been instrumental in finding similarities between molecules to discover new drugs [14, 15]. Applications of graph theory to chemical reaction networks have allowed the description and representation of complex reaction mechanisms using topological and complexity indices [16–22]. Reaction networks and graph theory have been used to study the dissociation of weak acids and bases. For example, the method of exponential polytopes has been employed to obtain approximate formulas for the pH of monoprotic weak acids [17]. Graph kernels have been utilized to estimate acid/base dissociation constants in molecules of biopharmaceutical interest [23]. Graph convolutional neural networks have been used for predicting the pK_a values and protonation state distribution of molecules of pharmaceutical interest [24]. In homogeneous catalysis, graph-theoretical methodology has allowed scientist to study the chemical reaction space of multicomponent mixtures [13]. In quantum chemistry, weighted-graph-theoretical approaches are used to compute contributions from many-body approximations in post-Hartree-Fock molecular dynamics [25].

In biochemistry, graph theory methods have been employed to analyze the covalent and non-covalent bond networks in proteins, allowing for the identification of flexible and rigid regions in these biomolecules [26]. Additionally, in biochemistry, graph convolutional networks have been used for automated function prediction of proteins from the protein structure [27]. Dynamical graph analysis of the hydrogen bond network has allowed to study structural changes in membrane proteins, and the identification of protein groups relevant for proton transfer activity [28]. In molecular biology, significant research has utilized graph theory and discrete mathematics to explore the relationship between sequence, structure, and function in biological molecules [29]. Graph theory methods have been particularly effective in analyzing RNA secondary structures, providing insights into their functional roles and interactions [30]. Furthermore, graph-theoretical complexes have been used to model DNA self-assembly of nanoscale geometric constructs, yielding promising results for future

nanotechnological applications in drug delivery, biosensors, and biomolecular computing [31].

Algebraic graph theory applies algebraic methods to graphs [32]. The connection between graphs and group theory is one of the main branches of algebraic graph theory [33]. The permutations of the vertices of a graph that maintain the edge-vertex connectivity endowed with the composition operation define the automorphism group of the graph. In chemistry, obtaining the automorphism group of a an associated graph is important in spectroscopy, quantum chemistry, structural elucidation and prediction of NMR spectrum of molecules, and in the characterization of molecular complexity, among other applications [34–38].

A polyprotic Brønsted-Lowry acid is a substance capable of donating more than one proton [39, 40]. These protons are released one by one in the consecutive (macroscopic) model, from the most acidic to the least acidic. The concentration of the chemical species involved in the consecutive dissociation model are obtained from the macroscopic equilibrium constants, the auto-ionization of water, and the balances of mass and charge of the acid dissolution [41–44]. In the non-consecutive (microscopic) dissociation model, the N protons are released independently. The concentrations of the chemical species involved in the non-consecutive dissociation are obtained from the micro-equilibrium constants, the auto-ionization of water, and the balances of charge and mass [45, 46]. Micro-equilibrium constants and concentrations are important in biochemistry and pharmaceutical sciences [47–53]. The relations between microscopic and macroscopic equilibrium constants of polyprotic acids were developed by Hill [54].

This work is organized as follows. Sections 2.1 and 2.2 are used to introduce the consecutive and non-consecutive acid dissociation models, respectively, along with the corresponding notation based on sets. Section 2.3 demonstrates that the use of a notation based on set theory simplifies the complicated expression obtained by Hill in terms of indices, allowing for a general expression to be derived for the micro-equilibrium constants. These are expressed in terms of the equilibrium constants and the molar fractions of the tautomers of the acid’s dissociation states. Examples of the diprotic and triprotic acids are provided in Section 2.5.

In Section 2.6, the use of graph theory to represent the microdissociation of polyprotic acids and to obtain their graph automorphism group is explored. The aqueous dissociation of N -protic acids, with $N = 1, 2, \dots, 6$ is thoroughly examined, identifying $\text{Aut}(G_N) = C_2 \times S_N$, as the automorphism group of these N -protic acid dissociation.

2 Theory and Methods

2.1 Consecutive dissociation of polyprotic acids

The aqueous dissociation equilibrium of a polyprotic weak acid H_NB is given by N consecutive acid dissociations plus the water auto-ionization,



respectively. The equilibria displayed by equations (1) and (2) are effective equilibria since the N protons of H_NB can dissociate separately and not necessarily consecutively [45, 46, 51].

The acid H_NB has $N + 1$ deprotonation states (DS)

$$\text{Z}_{\nu} = \text{H}_{N-\nu}\text{B}^{\nu-}, \quad \nu = 0, 1, 2, \dots, N, \quad (3)$$

with $\text{Z}_0 = \text{H}_N\text{B}$ as the fully protonated state, and $\text{Z}_N = \text{B}^{N-}$ as the fully deprotonated state. The activities of the DSs Z_{ν} are given by $a_{\nu}(\text{Z}_{\nu}) = \gamma_{\nu}[\text{Z}_{\nu}]/C^{\circ}$, with γ_{ν} as the molar activity coefficient, $[\text{Z}_{\nu}]$ as the molar concentration, and $C^{\circ} = 1 \text{ M}$. The activities of the hydronium and hydroxide ions are given by $a(\text{H}_3\text{O}^+) = \gamma_{\text{H}_3\text{O}^+}[\text{H}_3\text{O}^+]/C^{\circ}$ and $a(\text{OH}^-) = \gamma_{\text{OH}^-}[\text{OH}^-]/C^{\circ}$, with $[\text{H}_3\text{O}^+]$ and $[\text{OH}^-]$ as the molar concentrations of the hydronium and hydroxide ions.

The equilibrium state of a N -protic acid at analytical concentration C_a is mathematically characterized by $N + 3$ equations: the N equilibrium constants, the water autoionization

constant, and the balances of charge and mass

$$K_\nu = \frac{a(Z_\nu)a(\text{H}_3\text{O}^+)}{a(Z_{\nu-1})}, \quad \nu = 1, 2, \dots, N, \quad (4)$$

$$K_w = a(\text{H}_3\text{O}^+)a(\text{OH}^-), \quad (5)$$

$$[\text{H}_3\text{O}^+] = [\text{OH}^-] + \sum_{\nu=0}^N \nu [\text{Z}_\nu], \quad (6)$$

$$C_a = \sum_{\nu=0}^N [\text{Z}_\nu], \quad (7)$$

respectively. In the case of diluted solutions, it is valid to use the approximations $a(Z_\nu) \approx [\text{Z}_\nu]/C^\circ$, $a(\text{H}_3\text{O}^+) \approx [\text{H}_3\text{O}^+]/C^\circ$, and $a(\text{OH}^-) \approx [\text{OH}^-]/C^\circ$. The use of the biochemical standard state, $C^\ominus = 10^{-7}C^\circ$, to define the dimensionless quantities $z_\nu = [\text{Z}_\nu]/C^\ominus$, $x = [\text{H}_3\text{O}^+]/C^\ominus$, and $y = [\text{OH}^-]/C^\ominus$, allows to rewrite equations (4) to (7) as

$$k_\nu = \frac{z_\nu x}{z_{\nu-1}}, \quad \nu = 1, 2, \dots, N, \quad (8)$$

$$1 = xy, \quad (9)$$

$$x = y + \sum_{\nu=0}^N \nu z_\nu, \quad (10)$$

$$c_a = \sum_{\nu=0}^N z_\nu, \quad (11)$$

with $c_a = C_a/C^\ominus$, $k_w = 1$, and $k_\nu = 10^7 K_\nu$.

This N -protic acid has N distinguishable sites, each capable of being either occupied by a proton or left unoccupied. In this context, the dissociation state Z_ν is characterized by having $N - \nu$ occupied sites and ν unoccupied sites. The sites of H_NB are in one-to-one correspondence with the elements of the set $\mathbb{S}_N = \{1, 2, \dots, N\}$.

There are two distinct deprotonation schemes: consecutive and non-consecutive. In consecutive or sequential acid dissociation, protons on the occupied sites are released in a specific, predetermined order. Formally, this order is given by an enumeration of \mathbb{S}_N ,

$\mathcal{E} = (\nu_1, \nu_2, \dots, \nu_N)$, where

$$\begin{aligned}\nu_1 &\in \mathbb{S}_N, \\ \nu_2 &\in \mathbb{S}_N - \{\nu_1\}, \\ \nu_3 &\in \mathbb{S}_N - \{\nu_1, \nu_2\}, \dots, \\ \nu_n &\in \mathbb{S}_N - \{\nu_1, \nu_2, \dots, \nu_{n-1}\}, \dots, \\ \nu_N &\in \mathbb{S}_N - \{\nu_1, \nu_2, \dots, \nu_{N-1}\}.\end{aligned}$$

In the consecutive dissociation there is a one-to-one mapping between the states Z_μ and the sets $\mathbb{S}_N - \{\nu_1, \nu_2, \dots, \nu_\mu\}$, with Z_0 mapped to \mathbb{S}_N , Z_1 mapped to $\mathbb{S}_N - \{\nu_1\}$, \dots , Z_{N-1} mapped to $\mathbb{S}_N - \{\nu_1, \nu_2, \dots, \nu_{N-1}\}$, and Z_N mapped to \emptyset .

2.2 Nonconsecutive dissociation of polyprotic acids

On the other hand, in non-consecutive acid dissociation, the protons can separate independently instead of consecutively. Dissociation micro-states (DMSs) are necessary to describe the non-consecutive acid dissociation. In the non-consecutive dissociation, the dissociation state Z_ν has $\binom{N}{\nu} = \frac{N!}{(N-\nu)!\nu!}$ possible dissociation micro-states. these DMSs are given by the subsets of \mathbb{S}_N with $N - \nu$ elements. The set of micro-states of Z_ν is given by

$$M_\nu = \{U \in \mathcal{P}(\mathbb{S}_N) : |U| = N - \nu\}, \quad (12)$$

with $\mathcal{P}(\mathbb{S}_N)$ as the power set of \mathbb{S}_N , defined as:

$$\mathcal{P}(\mathbb{S}_N) = \{U : U \subseteq \mathbb{S}_N\}. \quad (13)$$

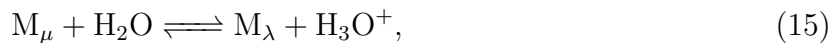
In simpler terms, M_ν represents the collection of all subsets of \mathbb{S}_N with $N - \nu$ elements, each corresponding to a unique DMS of Z_ν . The DMSs of Z_ν are given by M_μ with

$\mu \in M_\nu$. For example, the DS Z_1 of a 3-protic acid has $\binom{3}{1} = 3$ DMSs M_μ , with $\mu \in M_1 = \{\{1, 2\}, \{1, 3\}, \{2, 3\}\}$. The fully protonated and fully deprotonated state Z_0 and Z_N respectively, have only one DMS each $M_{\mathbb{S}_N}$ and M_\emptyset , respectively. An N -protic acid has a total of 2^N DMSs.

The molar concentration of the deprotonation state Z_ν , $[Z_\nu]$, is related to the molar concentrations of its deprotonation microstates, $[M_\mu]$, by

$$[Z_\nu] = \sum_{\mu \in M_\nu} [M_\mu], \quad \nu \in \mathbb{S}_N. \quad (14)$$

The deprotonation and protonation micro-equilibria (DMEs and PME, respectively) between the DMSs M_μ and M_λ are possible when the absolute difference between the sets μ and λ is 1, and either $\mu \subsetneq \lambda$ or $\lambda \subsetneq \mu$. These micro-equilibria are given by the chemical equations



and the micro-equilibrium constants

$$K_{\mu\lambda} = \frac{a(M_\lambda)a(\text{H}_3\text{O}^+)}{a(M_\mu)}, \quad (17)$$

$$K_{\lambda\mu} = \frac{a(M_\mu)a(\text{OH}^-)}{a(M_\lambda)}. \quad (18)$$

The activities of M_μ , M_λ , H_3O^+ and OH^- , are given by

$$\begin{aligned} a(M_\mu) &= \gamma_\mu [M_\mu]/C^\circ, & a(M_\lambda) &= \gamma_\lambda [M_\lambda]/C^\circ, \\ a(\text{H}_3\text{O}^+) &= \gamma_{\text{H}_3\text{O}^+} [\text{H}_3\text{O}^+]/C^\circ, \text{ and} & a(\text{OH}^-) &= \gamma_{\text{OH}^-} [\text{OH}^-]/C^\circ, \end{aligned}$$

respectively, with $C^\circ = 1 \text{ M}$ as the standard state, and γ_μ , γ_λ , $\gamma_{\text{H}_3\text{O}^+}$, and γ_{OH^-} , as the

activity coefficients. The addition of the chemical equations (15) and (16) gives the water autoionization equilibrium



which has equilibrium constant

$$\begin{aligned} K_w &= K_{\mu\lambda}K_{\lambda\mu} \\ &= a(\text{H}_3\text{O}^+)a(\text{OH}^-). \end{aligned} \quad (20)$$

Although the number of micro-equilibrium constants between the DMSs of $Z_{\nu-1}$ and Z_ν is given by $2\binom{N}{\nu-1}\binom{N}{\nu}$, only $2\binom{N}{\nu}(N-\nu)$ are chemically related. The set of chemically related DME constants is given by

$$K = \{K_{\mu\lambda} : \mu \subsetneq \lambda \text{ or } \lambda \subsetneq \mu, \text{abs}(|\mu| - |\lambda|) = 1\}. \quad (21)$$

The total number of DMEs and PMSs for a N -protic acid is given by $2^N N$. The 3-protic acid can be used as an example. The DMSs of Z_1 and Z_2 are given by M_μ and M_λ respectively, with $\mu \in M_1$ and $\lambda \in M_2$ as elements of the sets $M_1 = \{\{2, 3\}, \{1, 3\}, \{1, 2\}\}$ and $M_2 = \{\{1\}, \{2\}, \{3\}\}$, respectively. Since $\{3\} \not\subset \{1, 2\}$, or $\{1, 2\} \not\subset \{3\}$, there are not DMEs between the DMSs $\{1, 2\}$ of Z_1 and $\{3\}$ of Z_2 . On the other hand, since $\{1\} \subsetneq \{1, 2\}$, and $\text{abs}(|\{1, 2\}| - |\{1\}|) = 1$, there are DMEs and PMSs between $\{1, 2\}$ and $\{1\}$. In the particular case of a 3-protic acid, the total number of DMEs and PMSs is $3 \times 2^3 = 24$.

In the case of aqueous dilute solutions all the activity coefficients are approximately one, and it is justified to use the approximations $a(M_\mu) \approx [M_\mu]/C^\circ$, $a_{\text{OH}^-} \approx [\text{OH}^-]/C^\circ$, and $a_{\text{H}_3\text{O}^+} \approx [\text{H}_3\text{O}^+]/C^\circ$. The use of the biochemical standard state $C^\circ = 10^{-7}C^\circ$, allows to

write the micro-equilibrium constants (17), (18), and (20) as

$$k_{\mu\lambda} = \frac{xm_\lambda}{m_\mu}, \quad (22)$$

$$k_{\lambda\mu} = \frac{ym_\mu}{m_\lambda}, \quad (23)$$

$$1 = xy, \quad (24)$$

respectively. It can be shown that $k_{\mu\lambda} = 10^7 K_{\mu\lambda}$ and $k_{\lambda\mu} = 10^7 K_{\lambda\mu}$.

2.3 Relation between dissociation equilibria and micro-equilibria

There is a simple relation between the deprotonation equilibrium constants k_ν , with $\nu \in \mathbb{S}_N$, and the deprotonation micro-equilibrium constants, $k_{\mu\lambda}$, with $\mu \in M_{\nu-1}$, and $\lambda \in M_\nu$. The deprotonation equilibrium constant k_ν ,

$$k_\nu = \frac{xz_\nu}{z_{\nu-1}}, \quad \nu \in \mathbb{S}_N, \quad (25)$$

can be written in terms of the deprotonation micro-states

$$k_\nu = \frac{x \sum_{m_\lambda \in M_\nu} m_\lambda}{\sum_{m_\mu \in M_{\nu-1}} m_\mu}. \quad (26)$$

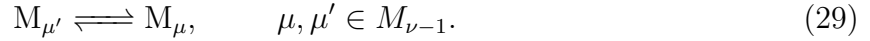
The reciprocal of k_ν is given by

$$\begin{aligned} \frac{1}{k_\nu} &= \sum_{\mu \in M_{\nu-1}} \frac{m_\mu}{x \sum_{\lambda \in M_\nu} m_\lambda} \\ &= \sum_{\mu \in M_{\nu-1}} \left(\sum_{\lambda \in M_\nu} \frac{xm_\lambda}{m_\mu} \right)^{-1} \\ &= \sum_{\mu \in M_{\nu-1}} \left(\sum_{\lambda \in M_\nu} k_{\mu\lambda} \right)^{-1}. \end{aligned} \quad (27)$$

A simpler relation between the equilibrium constants k_ν and the micro-equilibrium constants can be obtained by dividing numerator and denominator of the right hand side of equation (26) by $m_{\mu'}$ with $\mu' \in M_{\nu-1}$,

$$\begin{aligned} k_\nu &= \frac{x \sum_{\lambda \in M_\nu} m_\lambda / m_{\mu'}}{\sum_{\mu \in M_{\nu-1}} m_\mu / m_{\mu'}} \\ &= \frac{\sum_{\lambda \in M_\nu} k_{\mu'\lambda}}{\sum_{\mu \in M_{\nu-1}} \tau_{\mu'\mu}}, \end{aligned} \quad (28)$$

with $\tau_{\mu'\mu} = m_\mu / m_{\mu'}$ as the equilibrium constant for the tautomerization (isomerization) between the protonation micro-states M_μ and $M_{\mu'}$ of $Z_{\nu-1}$,



Equation (28) can be written in terms of the molar fractions $x_\mu = m_\mu / z_\nu$ for $\mu \in M_\nu$,

$$k_\nu = x_\mu \sum_{\lambda \in M_\nu} k_{\mu\lambda}, \quad \mu \in M_{\nu-1}. \quad (30)$$

It is easy to verify that the micro-equilibrium and tautomerization constants are related by:

$$k_{\mu'\lambda} = \tau_{\mu'\mu} k_{\mu\lambda}, \quad (31)$$

$$k_{\mu\lambda'} = k_{\mu\lambda} \tau_{\lambda\lambda'}. \quad (32)$$

An expression for the micro-equilibrium constants, in terms of the equilibrium constants and the microscopic molar fractions, can be obtained from the general definition of the microdissociation constants, $k_{\mu\lambda} = x m_\lambda / m_\mu$, for $\mu \in M_{\nu-1}$ and $\lambda \in M_\nu$. Multiplying the numerator of this expression by the unity $1 = z_\nu / z_\nu$, and the denominator by the unity $1 = z_{\nu-1} / z_{\nu-1}$, gives after rearranging terms

$$k_{\mu\lambda} = \frac{x_\lambda}{x_\mu} k_\nu, \quad \mu \in M_{\nu-1}, \lambda \in M_\nu. \quad (33)$$

This expression has been used previously, for the diprotic acid, in order to get the micro-equilibrium constants from the equilibrium constants and measurements of ^{13}C NMR [55].

2.4 Graph-Theory description of polyprotic acids microdissociation

In graph theory, a graph $G = (V, E)$ is a structure built from a set of vertices V , and a set of edges, E . The elements of E are the relations between pairs of vertices. Directed and undirected edges indicate one-way and two-way relationships between two vertices, respectively. Directed edges are written in parenthesis meanwhile undirected edges are written in curly brackets.

The dissociation of a N -protic acid can be represented by a graph $G_N = (V_N, E_N)$, with $V_N = \{M_\mu : \mu \in \mathcal{P}(\mathbb{S}_N)\}$, and E_N given by the set $E_N = R_N \cup T_N$ with

$$R_N = \{\{M_\mu, M_\lambda\}, \mu, \lambda \in \mathcal{P}(\mathbb{S}_N) : \mu \subsetneq \lambda \text{ or } \lambda \subsetneq \mu, \text{abs}(|\mu| - |\lambda|) = 1\}, \quad (34)$$

$$T_N = \{\{M_\mu, M_\lambda\}, \mu, \lambda \in \mathcal{P}(\mathbb{S}_N) : |\mu| = |\lambda| = |\mu \cap \lambda| + 1\}, \quad (35)$$

where R_N is the set of pairs of DMSs related by micro-equilibrium constants, and T_N is the set of pairs of DMSs related by tautomerization constants. The set T_N is the union of the tautomerization sets of each dissociation state Z_ν ,

$$T_N = \bigcup_{\nu=1}^{N-1} T_\nu, \quad (36)$$

$$T_\nu = \{\{M_\mu, M_\lambda\}, \mu, \lambda \in M_\nu : |\mu| = |\lambda| = |\mu \cap \lambda| + 1\},$$

with $T_\emptyset = T_{\mathbb{S}_N} = \emptyset$.

The microequilibrium and tautomerization constants of acid dissociation always occur in pairs. For every $k_{\mu\lambda}$ and $\tau_{\mu\mu'}$, there exist $k_{\lambda\mu}$ and $\tau_{\mu'\mu}$, respectively. This pairing of constants allows undirected edges to represent pairs of equilibrium and tautomerization constants in

the graph G_N .

A graph automorphism of G_N is a permutation, denoted σ , of the set of vertices, V_N , that maintains the edge-vertex connectivity of G_N . Because the compositions of two permutations is also a permutation, the composition of two graph automorphisms must likewise be a graph automorphism. The set of automorphisms of G_N , equipped with the composition of automorphisms, constitutes a group known as the graph automorphism group of G_N , denoted $\text{Aut}(G_N)$.

2.5 Relation between equilibrium and micro-equilibrium constants for diprotic and triprotic acids

In the case of a diprotic, acid the concentration vectors of dissociation and microdissociation states are $\mathbf{z}^\top = \{z_0, z_1, z_2\}$, and

$$\begin{aligned} \mathbf{m}^\top &= \{m_{\{1,2\}}, m_{\{2\}}, m_{\{1\}}, m_\emptyset\} \\ &= \{m_{12}, m_2, m_1, m_0\}, \end{aligned} \tag{37}$$

respectively. The second line of the equation defining \mathbf{m} was obtained by applying the assignation rules $\emptyset \rightarrow 0$, $\{1\} \rightarrow 1$, $\{2\} \rightarrow 2$, and $\{1,2\} \rightarrow 12$. In these terms, the vectors of dissociation and microdissociation constants are given by $\mathbf{k}^\top = \{k_1, k_2\}$, and $\tilde{\mathbf{k}}^\top = \{k_{12,1}, k_{12,2}, k_{1,0}, k_{2,0}\}$.

The use of equations (28), (31) and (32) produces the linear system of equations

$$k_1 = k_{12,1} + k_{12,2}, \tag{38}$$

$$k_2(1 + \tau) = k_{12,1}, \tag{39}$$

$$k_2(1 + \tau) = \tau k_{12,2}, \tag{40}$$

$$0 = \tau k_{10} - k_{20} \tag{41}$$

$$0 = k_{12,1} - \tau k_{12,2}, \tag{42}$$

where $\tau = \tau_{12}$. It is easy to verify that the combined use of these equations gives the dissociation constants, \mathbf{k} , in terms of the microdissociation constants, $\tilde{\mathbf{k}}$. The first dissociation constant is already given by equation (38), $k_1 = k_{12,1} + k_{12,2}$. The second dissociation constant is obtained by substitution of τ from equation (42) in equation (39) to obtain

$$k_2 = \frac{k_{12,1}k_{12,2}}{k_{12,1} + k_{12,2}}. \quad (43)$$

The microdissociation constants, $\tilde{\mathbf{k}}$, in terms of \mathbf{k} and τ are given by

$$\begin{aligned} k_{12,1} &= x_1 k_1, \\ k_{12,2} &= x_2 k_1, \\ k_{1,0} &= x_1^{-1} k_2, \\ k_{2,0} &= x_2^{-1} k_2, \end{aligned} \quad (44)$$

with $x_1 = m_1/z_1$ and $x_2 = m_2/z_1$.

The dissociation of the triprotic acid is a more interesting example. The concentration vector of dissociation states is $\mathbf{z} = \{z_0, z_1, z_2\}$. The concentration vector of the microdissociation states is

$$\mathbf{m}^\top = \{m_{S_3}, m_{23}, m_{13}, m_{12}, m_3, m_2, m_1, m_0\}. \quad (45)$$

The vectors of dissociation constants \mathbf{k} , and microdissociation constants $\tilde{\mathbf{k}}$, are given by $\mathbf{k}^\top = \{k_1, k_2, k_3\}$ and

$$\begin{aligned} \tilde{\mathbf{k}}^\top &= \{k_{S_3,23}, k_{S_3,13}, k_{S_3,12}, k_{23,2}, k_{23,3}, k_{13,1}, k_{13,3}, k_{12,1}, k_{12,2}, \\ & k_{30}, k_{20}, k_{10}\}. \end{aligned} \quad (46)$$

There are three possible tautomerizations between the dissociation micro-states $M_2 = \{1, 2, 3\}$.

The use of equations (31) and (32) gives

$$\tau_{12} = \frac{k_{20}}{k_{10}} = \frac{k_{12,1}}{k_{12,2}}, \quad (47)$$

$$\tau_{13} = \frac{k_{30}}{k_{10}} = \frac{k_{13,1}}{k_{13,2}}, \quad (48)$$

$$\tau_{23} = \frac{k_{30}}{k_{20}} = \frac{k_{23,2}}{k_{23,3}}. \quad (49)$$

In the same way, there are three tautomerizations between the dissociation micro-states $M_1 = \{12, 13, 23\}$

$$\tau_{12,13} = \frac{k_{13,1}}{k_{12,1}} = \frac{k_{S_3,12}}{k_{S_3,13}}, \quad (50)$$

$$\tau_{12,23} = \frac{k_{23,2}}{k_{12,2}} = \frac{k_{S_3,12}}{k_{S_3,23}}, \quad (51)$$

$$\tau_{13,23} = \frac{k_{23,3}}{k_{13,3}} = \frac{k_{S_3,13}}{k_{S_3,23}}. \quad (52)$$

The tautomerization constants are related by

$$\tau_{13} = \tau_{12}\tau_{23}, \quad (53)$$

$$\tau_{12,23} = \tau_{12,13}\tau_{13,23}. \quad (54)$$

The use of equation (28) with $\nu = 1$ gives the first dissociation constant of the triprotic acid $k_1 = k_{S_3,1} + k_{S_3,2} + k_{S_3,3}$. Equation (28) with $\nu = 2$ gives three equations for k_2 , which are all equivalent to

$$(1 + \tau_{12} + \tau_{13})k_2 = k_{12,1} + k_{13,1} + \tau_{12}k_{23,2}. \quad (55)$$

The use of the tautomerizations (47)-(49), in terms of the dissociation micro-states of Z_1 , gives

$$k_2 = \frac{k_{13,3}(k_{12,1}k_{12,2} + k_{13,1}k_{12,2} + k_{12,1}k_{23,2})}{k_{13,1}k_{12,2} + k_{12,1}k_{13,3} + k_{12,2}k_{13,3}}. \quad (56)$$

This is only one of three possible (equivalent) equations for k_2 . The third dissociation

constant of the triprotic acid gives also three equations equivalent to

$$(1 + \tau_{12,13} + \tau_{12,23})k_3 = k_{S_3,12}. \quad (57)$$

This equation gives $k_{S_3,12} = x_{12}^{-1}k_3$. The use of the tautomerizations (50)-(52), in terms of the dissociation micro-states of S_2 , in equation (57) gives

$$k_3 = \frac{k_{S_3,12}k_{S_3,13}k_{S_3,23}}{k_{S_3,12}k_{S_3,13} + k_{S_3,12}k_{S_3,23} + k_{S_3,13}k_{S_3,23}}. \quad (58)$$

Again, this is only one of three possible (equivalent) equations for k_3 .

The use of the tautomerizations (48) and(49) in $k_1 = k_{S_3,1} + k_{s_3,2} + k_{S_3,3}$ gives

$$k_{S_3,1} = \frac{k_1}{1 + \tau_{12} + \tau_{13}} = x_1k_1. \quad (59)$$

The constants $k_{S_3,2}$ and $k_{S_3,3}$ are obtained from equations (47) and (48)

$$k_{S_3,2} = \tau_{12}k_{S_3,1} = x_2k_1, \quad (60)$$

$$k_{S_3,3} = \tau_{13}k_{S_3,1} = x_3k_1. \quad (61)$$

The constant $k_{12,1}$ is obtained from equation (55) and the tautomerizations. The substitutions $k_{13,1} = \tau_{12,13}k_{12,1}$ and $\tau_{12}k_{23,2} = \tau_{12,23}k_{12,1}$ in (55) gives

$$k_{12,1} = \frac{1 + \tau_{12} + \tau_{13}}{1 + \tau_{12,13} + \tau_{12,23}}k_2 = \frac{x_{12}}{x_1}k_2. \quad (62)$$

The other constants of $\tilde{\mathbf{k}}$ are obtained from $k_{12,1}$ and the tautomerizations

$$k_{13,1} = \tau_{12,13}k_{12,1} = \frac{x_{13}}{x_1}k_2, \quad (63)$$

$$k_{12,2} = \frac{k_{12,1}}{\tau_{12}} = \frac{x_{12}}{x_2}k_2, \quad (64)$$

$$k_{23,2} = \frac{\tau_{12,23}}{\tau_{12}}k_{12,1} = \frac{x_{23}}{x_2}k_2, \quad (65)$$

$$k_{13,3} = \frac{\tau_{12,13}}{\tau_{13}}k_{12,1} = \frac{x_{13}}{x_3}k_2, \quad (66)$$

$$k_{23,3} = \frac{\tau_{12,23}}{\tau_{13}}k_{12,1} = \frac{x_{23}}{x_3}k_2. \quad (67)$$

Finally, the constants $k_{S_3,\mu}$, $\mu \in M_2$, are given by equation (57) and

$$k_{S_3,13} = \frac{1}{\tau_{12,13}}k_{S_3,12} = x_{13}^{-1}k_3, \quad (68)$$

$$k_{S_3,23} = \frac{1}{\tau_{12,23}}k_{S_3,12} = x_{23}^{-1}k_3. \quad (69)$$

2.6 Graph automorphism groups of the dissociation of polyprotic acids

In the case of a monoprotic acid, the sets V_1 and E_1 are $V_1 = \{M_1, M_0\}$ and $E_1 = \{\{M_1, M_0\}\}$. The monoprotic acid does not display tautomerizations. The graph $G_1 = (V_1, E_1)$ is depicted in Figure 1(a). This graph is known as the complete graph of order two, denoted as K_2 , where all vertices are connected by edges. The acid-base permutation

$$\sigma_{10} = (M_1M_0)(H_3O^+OH^-), \quad (70)$$

exchanges M_1 with M_0 , and H_3O^+ with OH^- . In terms of concentrations, σ_{10} exchanges m_1 with m_0 , and x with y . The effect of σ_{10} on the micro-equilibrium constants is given by $\sigma_{10}(k_{10}) = k_{01}$ and $\sigma_{10}(k_{01}) = k_{10}$. The graph G_1 is shown to be preserved under the action of σ_{10} in Figure 2. This means σ_{10} maps G_1 onto itself without losing edge connectivity, making

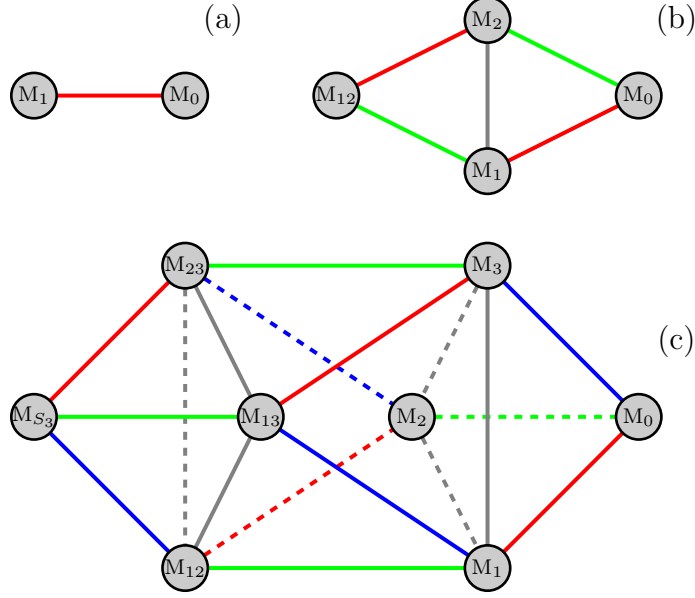


Figure 1: Dissociation graphs of some polyprotic acids. (a) Monoprotic acid; (b) Diprotic acid; (c) Triprotic acid. Red, green and blue edges represent the deprotonation/protonation of protons (1), (2), and (3), respectively, gray edges represent tautomerizations. Dashed edges are used to facilitate the visualization of G_3 .

σ_{10} a graph automorphism of G_1 . The identity permutation $e = (M_1)(M_0)(H_3O^+)(OH^-)$ is also a graph automorphism of G_1 . Under the operation of composition, the graph automorphisms e and σ_{10} generate the graph automorphism group of G_1 , denoted as $\text{Aut}(G_1) = \langle \sigma_{10} \rangle$. The permutation σ_{10} is an involution, meaning $\sigma_{10} = \sigma_{10}^{-1}$, hence $\sigma_{10}^2 = e$ establishes a condition on the generators of the group. The group presentation is given as

$$\text{Aut}(G_1) = \langle \sigma_{10} \mid \sigma_{10}^2 = e \rangle, \quad (71)$$

which specifies that the cyclic group of order two, C_2 , represents the monoprotic acid dissociation.

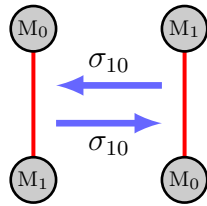


Figure 2: Effect of the permutations σ_{10} on the graph G_1 .

The dissociation of a diprotic acid is represented by the graph $G_2 = (V_2, E_2)$ with

$$V_2 = \{M_{12}, M_2, M_1, M_0\}, \quad (72)$$

$$E_2 = \{\{M_{12}, M_2\}, \{M_{12}, M_1\}, \{M_1, M_2\}, \{M_2, M_0\}, \{M_1, M_0\}\}. \quad (73)$$

The edge set is the union $E_2 = R_2 \cup T_2$ of the microdissociation set R_2 , and the tautomerization set $T_2 = \{\{M_1, M_2\}\}$. The graph $G_2 = (V_2, E_2)$ of the diprotic acid microdissociations is depicted in Figure 1(b). In this graph, red and green edges represent two types of microdissociations. The red edges correspond to the dissociations of protons occupying site 1, while the green edges correspond to protons at site 2. The gray edge represents the tautomerization between the DMSs M_1 and M_2 . The graph G_2 of the diprotic acid microdissociations is a complete tripartite graph, $G_2 = K_{1,1,2}$, also known as the diamond graph. The acid-base permutation $\sigma_{12,0}$, and the tautomerization permutation σ_{21} are defined as:

$$\sigma_{12,0} = (M_{12}M_0)(H_3O^+OH^-), \quad (74)$$

$$\sigma_{21} = (M_2M_1)(H_3O^+)(OH^-). \quad (75)$$

These permutations preserve the edge-vertex connectivity of G_2 , as shown in Figure 3. Under the composition operation, the graph automorphisms $\sigma_{12,0}$, σ_{21} , and the identity e , form the graph automorphism group of G_2 , denoted $\text{Aut}(G_2) = \langle \sigma_{12,0}, \sigma_{21} \rangle$. Since the permutations $\sigma_{12,0}$ and σ_{21} are involutions (self-inverses), the graph automorphism group of G_2 is given by

$$\text{Aut}(G_2) = \langle \sigma_{12,0}, \sigma_{21} \mid \sigma_{12,0}^2 = \sigma_{21}^2 = (\sigma_{12,0}\sigma_{21})^2 = e \rangle. \quad (76)$$

This is known as Klein's 4-group, or $C_2 \times C_2$. In Figure 3, it is evident that the product $\rho = \sigma_{12,0}\sigma_{21}$ results in a counterclockwise rotation of G_2 by π radians. Since C_2 and S_2 are isomorphic ($C_2 \cong S_2$), the automorphism group of the graph representing the diprotic acid is also expressed as $\text{Aut}(G_2) = C_2 \times S_2$.

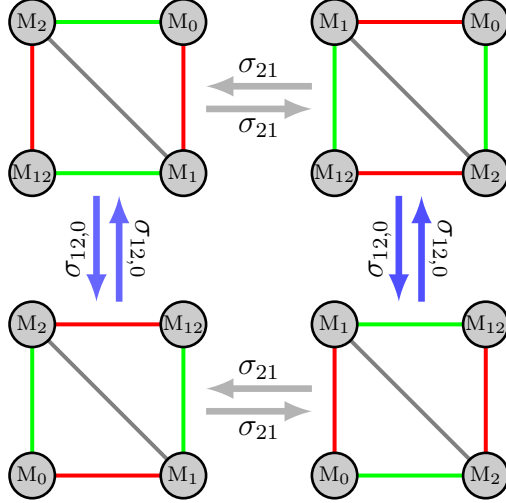


Figure 3: Effect of the permutations $\sigma_{12,0}$ and σ_{21} on the graph G_2 .

The triprotic acid dissociation is characterized by the sets V_3 and E_3

$$V_3 = \{M_\mu : \mu \in \mathcal{P}(\mathbb{S}_3)\}, \quad (77)$$

$$E_3 = R_3 \cup T_3, \quad (78)$$

where R_3 is the set of pairs of DMSs related by micro-equilibrium constants, and T_3 is the set of pairs of DMSs related by tautomerization constants. The graph $G_3 = (V_3, E_3)$ is shown in Figure 1(c). This graph displays three types of edges representing deprotonations: proton 1 in red, proton 2 in green, and proton 3 in blue. Tautomerizations are represented by gray edges. There are three permutations that serve as generators of the graph automorphism

group of G_3 :

$$\begin{aligned}\sigma_d &= \sigma_{12,23}\sigma_{1,2} \\ &= (M_{12}, M_{23})(M_1, M_2),\end{aligned}\tag{79}$$

$$\begin{aligned}\sigma'_d &= \sigma_{12,13}\sigma_{2,3} \\ &= (M_{12}, M_{13})(M_2, M_3),\end{aligned}\tag{80}$$

$$\begin{aligned}c_2 &= \sigma_{\mathbb{S}_3,0}\sigma_{12,1}\sigma_{13,2}\sigma_{23,3} \\ &= (M_{\mathbb{S}_3}, M_0)(M_{12}, M_{13})(M_{13}, M_2)(M_{23}, M_3)(\text{H}_3\text{O}^+\text{OH}^-),\end{aligned}\tag{81}$$

with σ_d and σ'_d as tautomerization permutations, and c_2 as an acid-base permutation. The presentation of this group is given by

$$\text{Aut}(G_3) = \langle \sigma_d, \sigma'_d, c_2 \mid \sigma_d^2 = (\sigma'_d)^2 = c_2^2 = e \rangle.\tag{82}$$

The effect of these permutations on G_3 is depicted in Figure 4. The permutations (79)-(81) can be interpreted as symmetry operations:

- The tautomerization σ_d acts as a reflection on the plane containing $M_{\mathbb{S}_3}$, M_{12} , M_3 , and M_0 .
- The tautomerization σ'_d is a reflection on the plane containing $M_{\mathbb{S}_3}$, M_{23} , M_1 , and M_0 .
- The acid-base permutation c_2 is a rotation about the axis that goes from the center of the graph through the midpoint between the DMSs M_{23} and M_3 .

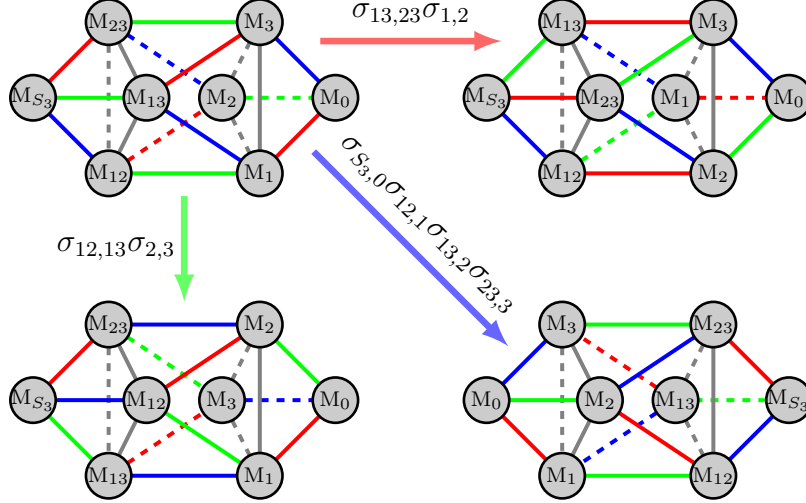


Figure 4: Effect of the permutations $\sigma_{13,23}\sigma_{1,2}$, $\sigma_{12,13}\sigma_{2,3}$, and $\sigma_{S_3,0}\sigma_{12,1}\sigma_{13,2}\sigma_{23,3}$, on the graph G_3 .

The other graph automorphisms of G_3 are

$$\sigma_d'' = (M_{12}, M_{23})(M_1, M_3), \quad (83)$$

$$c_3 = (M_{12}, M_{13}, M_{23})(M_1, M_3, M_2), \quad (84)$$

$$c_3^2 = (M_{12}, M_{23}, M_{13})(M_1, M_2, M_3), \quad (85)$$

$$c_2' = (M_0, M_{S_3})(M_{12}, M_2)(M_{13}, M_3)(M_{23}, M_1)(H_3O^+OH^-), \quad (86)$$

$$c_2'' = (M_0, M_{S_3})(M_{12}, M_3)(M_{13}, M_1)(M_{23}, M_2)(H_3O^+OH^-), \quad (87)$$

$$i = (M_0, M_{S_3})(M_{12}, M_3)(M_{13}, M_2)(M_{23}, M_1)(H_3O^+OH^-), \quad (88)$$

$$s_6 = (M_0, M_{S_3})(M_{12}, M_1, M_{13}, M_3, M_{23}, M_2)(H_3O^+OH^-), \quad (89)$$

$$s_6' = (M_0, M_{S_3})(M_{12}, M_2, M_{23}, M_3, M_{13}, M_1)(H_3O^+OH^-). \quad (90)$$

There are 12 permutations, the identity e and the 11 permutations given by Equations (79)–(81) and (83)–(90). These 12 permutations are divided in 6 tautomerizations and 6 acid-base permutations. The 6 tautomerizations are e , σ_d , σ_d' , σ_d'' , c_3 , and c_3^2 . The 6 acid-base permutations are c_2 , c_2' , c_2'' , i , s_6 , and s_6' .

The graph automorphisms (83)–(90) can be obtained by composition of the generators

σ_d , σ'_d , and c_2 . A simple inspection gives

$$c_3 = \sigma_d \sigma'_d, \quad (91)$$

$$c_3^2 = \sigma'_d \sigma_d, \quad (92)$$

$$\sigma''_d = c_3 \sigma_d = c_3^2 \sigma'_d, \quad (93)$$

$$s_6 = c_2 \sigma'_d = c'_2 \sigma_d, \quad (94)$$

$$s'_6 = c_2 \sigma_d, \quad (95)$$

$$c''_2 = i \sigma_d = s'_6 \sigma'_d, \quad (96)$$

$$i = c'_2 \sigma'_d. \quad (97)$$

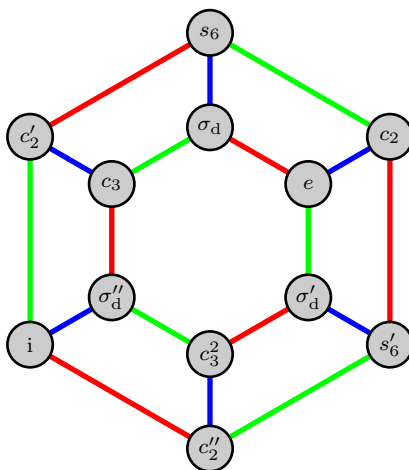


Figure 5: Cayley graph for the 3-protic acid dissociation. Red, green and blue edges represent the action of the generators σ_d , σ'_d , and c_2 , respectively.

In these compositions the product is taken from left to right. Other compositions, not shown here, also exist. A global view of the group $\text{Aut}(G_3)$, with presentation given by Equation (82), is given by the Cayley graph shown in Figure 5. This graph features two hexagonal cycles, both generated by σ_d and σ'_d , and connected by blue edges, c_2 . The inner hexagon consists solely of tautomerizations, while the outer hexagon comprises acid-base permutations. The set of tautomerizations H_T , and the set $H_C = \{e, c_2\}$, both contain the identity e , hence H_T and H_C are subgroups of $\text{Aut}(G_3)$. The subgroup H_T is generated by σ_d

and σ'_d , and is isomorphic to the symmetric group S_3 [56]. The subgroup H_C is generated by c_2 and is isomorphic to the cyclic group C_2 . The outer hexagon of the Cayley graph 5 is not a subgroup of $\text{Aut}(G_3)$, it is the left coset c_2H_T of H_T . It can be shown that $c_2H_R = H_Rc_2$, hence H_R is a normal subgroup of $\text{Aut}(G_3)$, $H_R \triangleleft \text{Aut}(G_3)$. Since C_2 is also a normal subgroup of $\text{Aut}(G_3)$, $\text{Aut}(G_3)$ is the direct product of S_3 and C_2 , $\text{Aut}(G_3) = S_3 \times C_2$. The 12 graph automorphisms, given by e and the permutations of Equations (79)–(81) and (83)–(90), are the elements of the group $\text{Aut}(G_3) = S_3 \times C_2$, which is isomorphic to $C_2 \times S_3$, and to the abstract dihedral group D_6 and the antiprismatic 3D point group D_{3d} (Schoenflies' notation).

The dissociation of the 4-protic acid is represented by the graph $G_4 = (V_4, E_4)$, with $V_4 = \{M_\mu : \mu \in \mathcal{P}(\mathbb{S}_4)\}$, and $E_4 = R_4 \cup T_4$. The set R_4 is the vertex set of DMSs related by micro-equilibrium constants, the set T_4 is the vertex set of pairs of DMSs related by tautomerization constants. The graph of the DMEs without tautomerizations, $G_{k,4} = (V_4, R_4)$, is shown in Figure 6, which is a hypercube graph Q_4 with $2^4 = 16$ vertices and $4 \times 2^{4-1} = 32$ edges. The graph of the tautomerizations, $G_{\tau,4} = (V_4, T_4)$, is shown in Figure 7, which is a disjoint graph made of two trivial graphs (K_1) for $M_{\mathbb{S}_4}$ and M_\emptyset , two tetrahedral graphs (K_4) for the DMSs of Z_1 and Z_3 , and one octahedral graph ($K_{2,2,2}$) for the DMSs of Z_2 .

The graph automorphism group $\text{Aut}(G_4)$ is obtained with the aid of Wolfram Mathematica 12 [57] through

$$\text{Aut}(G_4) = \text{GraphAutomorphismGroup}[\text{Graph}[\text{Hypercube}[4], \text{Graph}[\text{K4}, 2], \text{Graph}[\text{K4}, 2], \text{Graph}[\text{K2,2,2}], \text{Graph}[\text{K1}], \text{Graph}[\text{K1}]]], \quad (98)$$

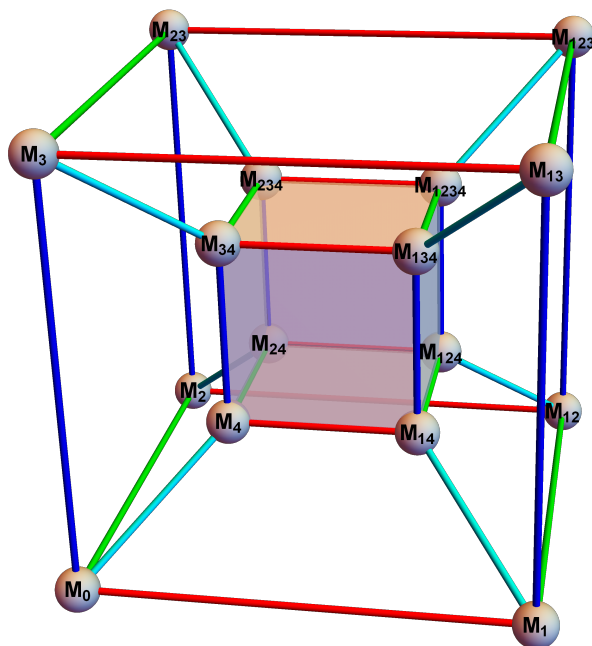


Figure 6: Graph $G_{k,4} = (V_4, R_4)$ of the DMEs of the 4-protic acid. Red, green, blue and cyan edges represent the deprotonation/protonation of protons (1), (2), (3), and (4), respectively.

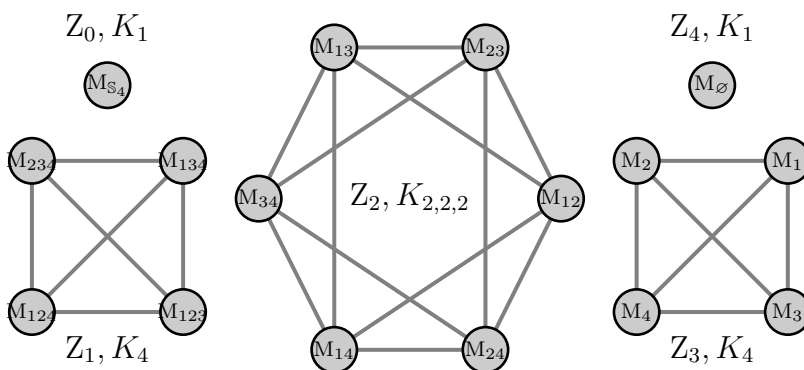


Figure 7: Graph $G_{\tau,4}$ of the tautomerizations of the 4-protic acid. This is a disjoint graph made of four subgraphs. M_{S_4} and M_0 are modeled by trivial graphs, the tautomers of Z_1 and Z_3 are modeled by tetrahedral graphs, finally the tautomerizations of Z_2 are modeled by the octahedral graph.

which gives a set of generators for $\text{Aut}(G_4)$:

$$\sigma_1 = (M_{124}, M_{134}) (M_{12}, M_{13}) (M_{24}, M_{34}) (M_2, M_3), \quad (99)$$

$$\sigma_2 = (M_{134}, M_{234}) (M_{13}, M_{23}) (M_{14}, M_{24}) (M_1, M_2), \quad (100)$$

$$\sigma_3 = (M_{123}, M_{124}) (M_{13}, M_{14}) (M_{23}, M_{24}) (M_3, M_4), \quad (101)$$

$$\sigma_4 = (M_{S_4}, M_\emptyset) (M_{123}, M_1) (M_{124}, M_2) (M_{134}, M_3) \quad (102)$$

$$(M_{234}, M_4) (M_{14}, M_{23}) (H_3O^+OH^-).$$

These permutations and the identity e generate a total of 48 group elements. The multiplication table (or Cayley table) of a group encodes all the information about the group's operation. Specifically, it shows how every pair of elements in the group combines under the group operation. Two groups are isomorphic if they have identical multiplication tables or if there exists a set of permutations of the elements of one group that transforms its multiplication table into a table identical to that of the other group [58]. The multiplication table of $\text{Aut}(G_4)$, \mathcal{M}_4 , is obtained using Mathematica 12 with the command:

$$\mathcal{M}_4 = \text{GroupMultiplicationTable}[\text{Aut}(G_4)]. \quad (103)$$

The multiplication table of the direct product group $C_2 \times S_4$ is obtained with the command:

$$\begin{aligned} \mathcal{M}_{C_2 \times S_4} = & \text{FiniteGroupData}[\\ & \{\text{"DirectProduct"}, \{\{\text{"CyclicGroup"}, 2\}, \{\text{"SymmetricGroup"}, 4\}\}\}, \\ & \text{"MultiplicationTable"}]. \end{aligned} \quad (104)$$

The elements of these matrices are integer numbers ranging from 1 to 48, each representing an element of the respective groups. Figure 8 displays the multiplication tables \mathcal{M}_4 and $\mathcal{M}_{C_2 \times S_4}$, visualized using Mathematica's `MatrixPlot` function with a hue-based color

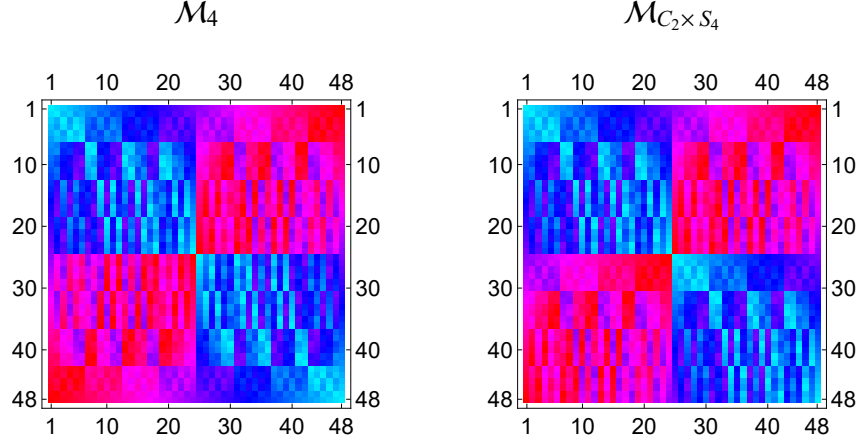


Figure 8: **MatrixPlot** of the multiplication tables of $\text{Aut}(G_4)$, \mathcal{M}_4 , and of the direct product $C_2 \times S_4$, $\mathcal{M}_{C_2 \times S_4}$.

scheme. These multiplication tables each consist of four blocks. All the blocks in $\mathcal{M}_{C_2 \times S_4}$ and the two top blocks in \mathcal{M}_4 are isomorphic to the Cayley table of the group S_4 , \mathcal{M}_{S_4} . The bottom blocks of \mathcal{M}_4 can be transformed into the corresponding blocks of $\mathcal{M}_{C_2 \times S_4}$ by reversing the rows and columns within each block. More precisely, there exists a permutation matrix \mathbf{P} that transforms the bottom blocks of \mathcal{M}_4 into matrices isomorphic to \mathcal{M}_{S_4} after a suitable renaming of the elements. This matrix \mathbf{P} is given by the 2×2 block matrix

$$\mathbf{P} = \begin{pmatrix} \mathbf{I}_{24} & \mathbf{0}_{24} \\ \mathbf{0}_{24} & \mathbf{J}_{24} \end{pmatrix}. \quad (105)$$

In this matrix, \mathbf{I}_{24} and $\mathbf{0}_{24}$ are the 24×24 identity and zero matrices, respectively, and \mathbf{J}_{24} is the 24×24 exchange matrix given by

$$\mathbf{J}_{24} = \delta_{i,25-j}, \quad 1 \leq i, j \leq 24, \quad (106)$$

with $\delta_{i,j}$ as the Kronecker delta which is 1 if $i = j$ and zero otherwise. The matrix \mathbf{P}

transforms \mathcal{M}_4 into \mathcal{M}'_4 using the equation

$$\mathcal{M}'_4 = \mathbf{P}\mathcal{M}_4\mathbf{P}^\top. \quad (107)$$

Next, by applying the relabeling rule

$$\mathcal{R} = \{48 \rightarrow 25, 47 \rightarrow 26, \dots, 25 \rightarrow 48\}, \quad (108)$$

the matrix \mathcal{M}'_4 is converted into \mathcal{M}''_4 which is isomorphic to $\mathcal{M}_{C_2 \times S_4}$. Consequently $\text{Aut}(G_4) \cong C_2 \times S_4$, which is isomorphic to the octahedral group O_h .

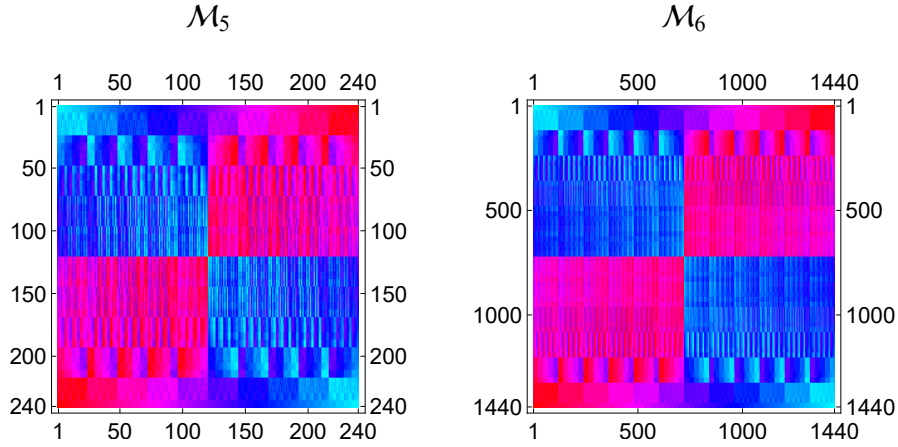


Figure 9: MatrixPlot of the Cayley tables of the groups $\text{Aut}(G_5)$ and $\text{Aut}(G_6)$.

The Cayley tables for $\text{Aut}(G_5)$ and $\text{Aut}(G_6)$, denoted \mathcal{M}_5 and \mathcal{M}_6 respectively, are shown in the Figure 9. These tables exhibit a similar pattern to the Cayley table \mathcal{M}_4 represented in Figure 8. The Cayley tables for the symmetric groups S_5 and S_6 can be generated in Mathematica 12 using the command:

$$\mathcal{M}_{S_n} = \text{GroupMultiplicationTable}[\text{SymmetricGroup}[n]], \quad (109)$$

with $n = 5, 6$. The top blocks of \mathcal{M}_5 and \mathcal{M}_6 are isomorphic to \mathcal{M}_{S_5} and \mathcal{M}_{S_6} respectively. There are specific matrices and renaming rules that transform the bottom blocks of \mathcal{M}_5 and

\mathcal{M}_6 into matrices isomorphic to \mathcal{M}_{S_5} and \mathcal{M}_{S_6} respectively. These matrices are given by

$$P_n = \begin{pmatrix} I_{n!} & 0_{n!} \\ 0_{n!} & J_{n!} \end{pmatrix}, \quad (110)$$

with $I_{n!}$ and $0_{n!}$ as the $n!$ -dimensional identity and zero matrices, and $J_{n!}$ as the $n!$ -dimensional exchange matrix explicitly defined by

$$J_{n!} = \delta_{i,1+n!-j}, \quad 1 \leq i, j \leq n!. \quad (111)$$

The renaming rules are given by

$$\mathcal{R}_n = \{2n! \rightarrow n! + 1, 2n! - 1 \rightarrow n! + 2, \dots, n! + 1 \rightarrow 2n!\}. \quad (112)$$

The use of these matrices and renaming rules on the multiplication tables \mathcal{M}_5 and \mathcal{M}_6 gives matrices \mathcal{M}_5'' and \mathcal{M}_6'' that are isomorphic to \mathcal{M}_{S_5} and \mathcal{M}_{S_6} , respectively.

It has been shown that for $N = 1, 2, \dots, 6$, the microdissociation of an N -protic acid has a graph G_N with graph automorphism group

$$\text{Aut}(G_N) \cong C_2 \times S_N. \quad (113)$$

The observed behavior is attributed to the interplay of two distinct equilibrium types: microdissociation and tautomerization. Microdissociation equilibria correlate with the C_2 component, while tautomerization equilibria are linked to the S_N component of the automorphism group.

Based on the underlying physics and chemistry of the microdissociation, we hypothesize that the graph representing this process has an automorphism group isomorphic to the direct product $C_2 \times S_N$.

3 Concluding remarks

The description of the microdissociation of an N -protic acid in terms of set theory is utilized to derive mathematical relations between equilibrium and micro-equilibrium dissociation constants. These mathematical relations are more convenient to use compared to the formulas based on indexation provided by Hill [54]. The advantages of our formalism are demonstrated by deriving equations that relate the equilibrium and micro-equilibrium constants of diprotic and triprotic acids.

Graph theory has been employed to represent and classify the microdissociation equilibrium of polyprotic acids as graphs, denoted as G_N , with the dissociation micro-states as vertices and the pairs of vertices connected by microdissociation constants as edges. Tautomerizations and acid-base reactions are treated as permutations on the vertex set of the polyprotic acid graph. It is shown that these permutations are graph automorphisms, and the composition of two of these permutations is also a graph automorphism. The set of automorphisms, endowed with composition, forms the automorphism group of the graph G_N . The generators of these groups were completely identified for monoprotic to 4-protic acids. In the case of monoprotic acids the graph automorphism group is given by the cyclic group $C_2 \cong S_2$. The analysis of the dissociation of a diprotic acid reveals the direct product $C_2 \times C_2$. An analysis of the Cayley graph of $\text{Aut}(G_3)$ allowed the identification of C_2 and S_3 as normal subgroups, leading to the conclusion that $\text{Aut}(G_3)$ is isomorphic to the direct product $C_2 \times S_3$. The Cayley tables of $\text{Aut}(G_4)$ and $C_2 \times S_4$, \mathcal{M}_4 and $\mathcal{M}_{C_2 \times S_4}$ respectively, were compared. These tables exhibit a 2×2 block structure, with the top blocks isomorphic to the multiplication table of the symmetric group \mathcal{M}_{S_4} . By permuting pairs of elements of \mathcal{M}_4 and renaming some elements, a multiplication table isomorphic to \mathcal{M}_{S_4} was obtained, confirming that $\text{Aut}(G_4)$ is isomorphic to the direct product $C_2 \times S_4$. Furthermore, the multiplication tables of the graph automorphism groups of the 5-protic and 6-protic acids were compared to those of the symmetric groups S_5 and S_6 . The same block structure observed in \mathcal{M}_4 was found in these comparisons. Computational verification confirmed that each of

the four blocks of these multiplication tables is isomorphic to either \mathcal{M}_{S_5} or \mathcal{M}_{S_6} , indicating that $\text{Aut}(G_N) \cong C_2 \times S_N$ for $N = 1, 2, \dots, 6$.

The computational proof for the 6-protic acid is particularly significant due the unique nature of the automorphism group of S_6 [59, 60]. The automorphism group of S_6 is isomorphic to the semidirect product $S_6 \rtimes C_2$, which includes an additional outer automorphism beyond the inner automorphisms derived from S_6 's elements. It is important to note that the multiplication table of S_6 captures only the inner automorphisms, reflecting how elements relate through conjugation, and does not account for the outer automorphism present in $\text{Aut}(S_6)$. Since the 4 blocks of the multiplication table \mathcal{M}_6 are isomorphic to the multiplication table \mathcal{M}_{S_6} , the outer automorphism is irrelevant for our purposes, as the table primarily highlights the inner group structure, not additional symmetries introduced by outer automorphisms.

The formalism and results presented in this paper contribute to advance our comprehension of acid-base equilibria and provide a foundation for future investigations into more complex chemical systems, such as biochemical and macromolecular processes.

Author Contributions

CAA led the conceptualization, formal analysis, funding acquisition, investigation, model development, and writing of the original draft. NS and JL handled data curation, investigation, computer program design, and figure creation, and they also assisted with text revision.

Conflict of Interest

No potential conflict of interest was reported by the authors.

4 Acknowledgments

This work has been partially funded by OMICAS Program: In-silico Multiscale Optimization of Sustainable Agricultural Crops (Infrastructure and validation in Rice and Sugar Cane) sponsored within the Scientific Colombia Ecosystem, made up by the World Bank, Ministry of Science, Technology, and Innovation (Minciencias), Icetex, Ministry of Education and Ministry of Industry and Tourism, Project ID: FP44842-217-2018. Partial funding was also provided by the internal research grants of Universidad Icesi.

The authors express their sincere gratitude to Professor Mathew Macauley of Clemson University for his invaluable insights and generous correspondence regarding group theory and graphical representation of groups.

Data Availability Statement

The results of this work are mainly analytical. Codes to produce the figures and Wolfram Mathematica Notebooks are available at <https://github.com/caarango/TizZ-codes-> or can be obtained by request from the corresponding author.

References

- (1) Cayley LVII. On the mathematical theory of isomers. *The London, Edinburgh, and Dublin Philosophical Magazine and Journal of Science* **1874**, *47*, 444–447.
- (2) Cayley, F. R. S. On the Analytical Forms called Trees, with Applications to the Theory of Chemical combinations. *Rept. Brit. Assoc. Adv. Sci.* **1875**, *45*, 257.
- (3) Brunel, G. Polymérisation du carbone. *Proc-verb. soc. Sci. Phys. Nat. Bordeaux* **1894**, 8–10.
- (4) Brunel, G. Sur la représentation graphique des isomères. *Proc-verb. soc. Sci. Phys. Nat. Bordeaux* **1898**, 108–110.
- (5) Rouvray, D. H. Isomer enumeration methods. *Chem. Soc. Rev.* **1974**, *3*, 355–372.

- (6) Rouvray, D. The pioneering contributions of Cayley and Sylvester to the mathematical description of chemical structure. *Journal of Molecular Structure: THEOCHEM* **1989**, *185*, 1–14.
- (7) Gutman, I. Georges Brunel - A Forgotten Pioneer of Chemical Graph Theory. *MATCH Commun. Math. Comput. Chem.* **2014**, *72*, 573–576.
- (8) Sylvester, J. J. On an Application of the New Atomic Theory to the Graphical Representation of the Invariants and Covariants of Binary Quantics, with Three Appendices. *American Journal of Mathematics* **1878**, *1*, 64–104.
- (9) Balaban, A. T., Ed. *Chemical Applications of Graph Theory*; Academic Press, 1976.
- (10) Trinajstić, N. *Chemical Graph theory*, 2nd ed.; CRC Press, 1992.
- (11) Bonchev, D., Rouvray, D. H., Eds. *Chemical group theory: introduction and fundamentals*; Mathematical Chemistry; Gordon and Breach Science Publishers, 1994; Vol. 3.
- (12) Bonchev, D., Rouvray, D. H., Eds. *Chemical group theory: techniques and applications*; Mathematical Chemistry; Gordon and Breach Science Publishers, 1994; Vol. 4.
- (13) Hashemi, A.; Bougueroua, S.; Gaigeot, M.-P.; Pidko, E. A. ReNeGate: A Reaction Network Graph-Theoretical Tool for Automated Mechanistic Studies in Computational Homogeneous Catalysis. *Journal of Chemical Theory and Computation* **2022**, *18*, 7470–7482, PMID: 36321652.
- (14) Droschinsky, A.; Humbeck, L.; Koch, O.; Kriege, N. M.; Mutzel, P.; Schäfer, T. In *Algorithms for Big Data: DFG Priority Program 1736*; Bast, H., Korzen, C., Meyer, U., Penschuck, M., Eds.; Springer Nature Switzerland: Cham, 2022; pp 76–96.
- (15) Branco, D.; Di Martino, B.; Cosconati, S.; Kranzmueller, D.; D’Angelo, S. Towards a Parallel Graph Approach to Drug Discovery. *Advanced Information Networking and Applications*. Cham, 2023; pp 127–135.
- (16) Clarke, B. L. Stability analysis of a model reaction network using graph theory. *The Journal of Chemical Physics* **1974**, *60*, 1493–1501.
- (17) Clarke, B. L. *Advances in Chemical Physics*; John Wiley & Sons, Ltd, 1980; pp 1–215.
- (18) Temkin, O. N.; Zeigarnik, A. V.; Bonchev, D. G. Application of Graph Theory to Chemical Kinetics. Part 2. Topological Specificity of Single-Route Reaction Mechanisms. *Journal of Chemical Information and Computer Sciences* **1995**, *35*, 729–737.

- (19) Temkin, O. N.; Zeigarnik, A. V.; Bonchev, D. *Chemical Reaction Networks: A graph-theoretical approach*; CRC Press, Taylor & Francis Group, 1996.
- (20) Zeigarnik, A. V.; Temkin, O. N.; Bonchev, D. Application of Graph Theory to Chemical Kinetics. 3. Topological Specificity of Multiroute Reaction Mechanisms. *Journal of Chemical Information and Computer Sciences* **1996**, *36*, 973–981.
- (21) Feinberg, M. *Foundations of Chemical Reaction Network Theory*; Springer, 2019.
- (22) Futamata, N.; Yamamura, R.; Trinh Ha, D.; Takahashi, O. Fragmentation pathways of methylbenzoate cations following core excitation: Theoretical approach using graph theory. *Chemical Physics Letters* **2021**, *766*, 138316.
- (23) Rupp, M.; Körner, R.; Tetko, I. V. Estimation of Acid Dissociation Constants Using Graph Kernels. *Molecular Informatics* **2010**, *29*, 731–740.
- (24) Johnston, R. C.; Yao, K.; Kaplan, Z.; Chelliah, M.; Leswing, K.; Seekins, S.; Watts, S.; Calkins, D.; Chief Elk, J.; Jerome, S. V.; Repasky, M. P.; Shelley, J. C. Epik: pKa and Protonation State Prediction through Machine Learning. *Journal of Chemical Theory and Computation* **2023**, *19*, 2380–2388, PMID: 37023332.
- (25) Zhang, J. H.; Ricard, T. C.; Haycraft, C.; Iyengar, S. S. Weighted-Graph-Theoretic Methods for Many-Body Corrections within ONIOM: Smooth AIMD and the Role of High-Order Many-Body Terms. *Journal of Chemical Theory and Computation* **2021**, *17*, 2672–2690, PMID: 33891416.
- (26) Jacobs, D. J.; Rader, A.; Kuhn, L. A.; Thorpe, M. Protein flexibility predictions using graph theory. *Proteins: Structure, Function, and Bioinformatics* **2001**, *44*, 150–165.
- (27) Gligorijević, V.; Renfrew, P. D.; Kosciolk, T.; Leman, J.; Berenberg, D.; Vatanen, T.; Chandler, C.; Taylor, B. C.; Fisk, I. M.; Vlamakis, H.; Xavier, R. J.; Knight, R.; Cho, K.; Bonneau, R. Structure-based protein function prediction using graph convolutional networks. *Nat. Commun.* **2021**, *12*, 3168.
- (28) Siemers, M.; Lazaratos, M.; Karathanou, K.; Guerra, F.; Brown, L. S.; Bondar, A.-N. Bridge: A Graph-Based Algorithm to Analyze Dynamic H-Bond Networks in Membrane Proteins. *Journal of Chemical Theory and Computation* **2019**, *15*, 6781–6798, PMID: 31652399.
- (29) Jonoska, N., Saito, M., Eds. *Discrete and Topological Models in Molecular Biology*; Natural Computing Series; Springer Berlin, Heidelberg, 2014.

- (30) Heitsch, C.; Poznanović, S. In *Discrete and Topological Models in Molecular Biology*; Jonoska, N., Saito, M., Eds.; Springer Berlin, Heidelberg, 2014; pp 145–166.
- (31) Ellis-Monaghan, J.; Pangborn, G.; Beaudin, L.; Miller, D.; Bruno, N.; Hashimoto, A. In *Discrete and Topological Models in Molecular Biology*; Jonoska, N., Saito, M., Eds.; Springer Berlin, Heidelberg, 2014; pp 241–270.
- (32) Godsil, C.; Royle, G. *Algebraic graph theory*; Springer, 2001.
- (33) Biggs, N. *Algebraic graph theory*, 2nd ed.; Cambridge University Press, 1993.
- (34) Razinger, M.; Balasubramanian, K.; Munk, M. E. Graph automorphism perception algorithms in computer-enhanced structure elucidation. *Journal of Chemical Information and Computer Sciences* **1993**, *33*, 197–201, PMID: 8314927.
- (35) Balasubramanian, K. Computational Techniques for the Automorphism Groups of Graphs. *Journal of Chemical Information and Computer Sciences* **1994**, *34*, 621–626.
- (36) Balasubramanian, K. Graph theoretical perception of molecular symmetry. *Chemical Physics Letters* **1995**, *232*, 415–423.
- (37) Randić, M. Aromaticity of Polycyclic Conjugated Hydrocarbons. *Chemical Reviews* **2003**, *103*, 3449–3606, PMID: 12964878.
- (38) Tratch, S.; Zefirov, N. Symmetry specified enumeration of substituted derivatives: an easy solution to the complex problem. *Russ. Chem. Bull.* **2008**, *57*, 235–252.
- (39) Petrucci, R.; Herring, F.; Madura, J.; Bissonnette, C. *Petrucci's General Chemistry: Modern Principles and Applications*, eBook; Pearson Education, 2023.
- (40) Atkins, P.; Jones, L. *Chemical Principles*; W. H. Freeman, 2008.
- (41) Harris, D.; Lucy, C. *Quantitative Chemical Analysis*, 10th ed.; W. H. Freeman, 2019.
- (42) Skoog, D. A.; West, D. M.; Holler, F. J.; Crouch, S. R. *Fundamentals of Analytical Chemistry*, 10th ed.; Cengage, 2021.
- (43) Denbigh, K. G. *The Principles of Chemical Equilibrium: With Applications in Chemistry and Chemical Engineering*, 4th ed.; Cambridge University Press, 1981.

- (44) Stumm, W.; Morgan, J. *Aquatic Chemistry: Chemical Equilibria and Rates in Natural Waters*; Environmental Science and Technology: A Wiley-Interscience Series of Textsand Monographs; Wiley, 2012.
- (45) Adams, E. Q. Relations Between the Constants of Dibasic Acids and of Amphoteric Electorolytes. *Journal of the American Chemical Society* **1916**, *38*, 1503–1510.
- (46) Mchedlov-Petrosyan, N. Polyprotic Acids in Solution: is the Inverse of the Constants of Stepwise Dissociation Possible? *Ukrainian Chemistry Journal* **2019**, *85*, 3–45.
- (47) Yatsimirskii, K. B.; Chekman, I. S.; Budarin, L. I.; Romanenko, É. D.; Frantsuzova, S. B. NMR Spectra and microequilibrium constants in izadrin (isadrine) and teranol solutions. *Theor. Exp. Chem.* **1978**, *13*, 262–267.
- (48) Noszal, B. Group constant: A measure of submolecular basicity. *The Journal of Physical Chemistry* **1986**, *90*, 4104–4110.
- (49) Hernández-Borrell, J.; Montero, M. T. Calculating Microspecies Concentration of Zwitterion Ampho-
teric Compounds: Ciprofloxacin as Example. *Journal of Chemical Education* **1997**, *74*, 1311.
- (50) Mazák, K.; Noszál, B. Advances in microspeciation of drugs and biomolecules: Species-specific con-
centrations, acid-base properties and related parameters. *Journal of Pharmaceutical and Biomedical
Analysis* **2016**, *130*, 390–403, Review Issue 2016.
- (51) Scholz, F.; Kahlert, H. Acid–base equilibria of amino acids: microscopic and macroscopic acidity con-
stants. *ChemTexts* **2018**, *4*.
- (52) Pála, T.; Fogarasi, E.; Noszál, B.; Tóth, G. Characterization of the Site-Specific Acid-Base Equilibria
of 3-Nitrotyrosine. *Chemistry & Biodiversity* **2019**, *16*, e1900358.
- (53) Li, G.; Wang, Y.; Sun, C.; Liu, F. Determination of the microscopic acid dissociation constant of
piperacillin and identification of dissociated molecular forms. *Frontiers in Chemistry* **2023**, *11*.
- (54) Hill, T. L. Microscopic Equilibria in Ampholytes. *Journal of the American Chemical Society* **1943**, *65*,
2119–2121.
- (55) Laufer, D. A.; Gelb, R. I.; Schwartz, L. M. Carbon-13 NMR determination of acid-base tautomerization
equilibriums. *The Journal of Organic Chemistry* **1984**, *49*, 691–696.

- (56) Nash, D. Cayley graphs of symmetric groups generated by reversals. *Pi Mu Epsilon Journal* **2005**, *33*, 143–147.
- (57) Wolfram Research, Inc. Mathematica, Version 12.0. <https://www.wolfram.com/mathematica>, Champaign, IL, 2019.
- (58) Carter, N. *Visual Group Theory*; Classroom resource materials; Mathematical Association of America, 2009.
- (59) Janusz, G.; Rotman, J. Outer Automorphisms of S_6 . *The American Mathematical Monthly* **1982**, *89*, 407–410.
- (60) Fournelle, T. A. Symmetries of the Cube and Outer Automorphisms of S_6 . *The American Mathematical Monthly* **1993**, *100*, 377–380.